ARTICLE IN PRESS

Synthesis of new rhodanine derivative molecules, their biological properties and sensor applications in environmental samples

Onur Cem Altunoluk[1,*], Oguz Özbek[2,*], Erbay Kalay[3,*], Caglar Berkel[2], Ömer Isildak[1]

[1]Tokat Gaziosmanpasa University, Faculty of Science and Arts, Department of Chemistry, 60250 Tokat, Turkey
[2]Tokat Gaziosmanpasa University, Faculty of Science and Arts, Department of Molecular Biology and Genetics, 60250 Tokat, Turkey
[3]Kafkas University, Kars Vocational School, Department of Material and Material Processing Technologies, 36100 Kars, Turkey
*E-mail: altunolukonurcem@gmail.com; oguz.ozbek@gop.edu.tr; erbaykalay@gmail.com

Abstract

In this study, two new rhodanine derivative molecules (**3** and **4**) were synthesized, and the potentiometric sensor properties and certain biological functions of these new molecules were investigated, following their characterization. The potentiometric performance characteristics of sensor 2 prepared using the molecule **3** and sensor 10 prepared using the molecule **4** were further investigated under laboratory conditions. The sensors in which new rhodanine derivative molecules were used as ionophores exhibited selectivity against Ba^{2+} ions among 19 different ions (Na^{+}, Li^{+}, K^{+}, Ca^{2+}, Mg^{2+}, Pb^{2+}, Cu^{2+}, Zn^{2+}, Co^{2+}, Sr^{2+}, Mn^{2+}, Ni^{2+}, Cd^{2+}, Cr^{3+}, Al^{3+}, Gd^{3+}, Nd^{3+} and In^{3+}). In the potential measurements performed using Ba^{2+} ion solutions, sensor 2 had a near–Nernstian response of 25.0±2.5 mV/decade and a detection limit of 7.66×10^{-7} M in the concentration range of 1.0×10^{-6}–1.0×10^{-1} M, while sensor 10 had a near–Nernstian response of 27.0±2.3 mV/decade and a detection limit of 9.77×10^{-8} M in the concentration range of 1.0×10^{-1}–1.0×10^{-7} M. Both sensors had a quick response time of 6 and 5 seconds, respectively; and sensor 10 was shown to be able work in a wider pH range (5.0–9.0) without being influenced by the changes in pH. Furthermore, both sensors exhibited a repeatable and stable behavior. The surface morphologies of the prepared potentiometric sensors were examined by scanning electron microscope (SEM). Ba^{2+} ion analysis was performed in different environmental water samples using sensor 10, and the newly fabricated sensor was found to be able to determine Ba^{2+} ions with very high recoveries. These novel rhodanine derivative molecules were also observed to have a slight growth inhibitory potential against particular bacterial species.

Keywords: Rhodanine, synthesis, sensor, antimicrobial activity, ionophore, barium(II), potentiometry

ARTICLE IN PRESS

1. Introduction

Barium is an alkaline earth metal and 14th most commonly found element on the Earth's crust with a concentration of approximately 500 ppm [1]. Barium constitutes around 0.03% of the Earth's crust, mainly as the minerals “Barite” (also known as barytes or heavy spar) and “Witherite”. The abundance of barium is 13 μg/l in seawater. Based on its high chemical reactivity, it is not present as a free element (never found free in nature), but found in the form of barium sulfate and barium carbonate. To date, barium has no known biological function in humans yet [2]. However, it was reported to be essential for the growth of some other organisms, including desmid green alga *Closterium moniliferum* which contain vesicles with barium sulfate in the crystalline form as barite [3]. Human uptake of barium is associated with the absorption mostly via food, and drinking water to a lesser extent. Most food products generally contain lower than 3mg/100g barium, with the exception of Brazilian nuts which contain 150–300 mg/100 g of barium. Barium concentration in drinking water shows high variability, based on the geographical area, but it is generally present in the order of tens of micrograms per liter [4]. Bread consumption alone contributes to the daily intake of barium by diet with a 20%. In tissues, mean barium levels are estimated to be approximately 20 mg [5]. The concentration of barium generally present in food and drinking water generally is not high enough to be considered as a health risk for humans. However, data is still being collected to identify the health effects of long-term exposure to low concentrations of barium. People having the highest known risk of exposure to high levels of barium are those employed in industries making or using barium compounds.

Barium is used in various industrial applications [6, 7]. Barium salts (nitrate and sulfate), are present in numerous products, such as ceramics, plastics, adhesives, paints, bricks, tiles, glass, rubber, insect and rat poisons, electronics, drugs, vinyl stabilizers, railroad flares, fireworks,

ARTICLE IN PRESS

additives to lubricating oil, permanent magnets, fine chemicals, in drilling fluids for oils and gas wells, as a molecule giving green color in fireworks by burning barium nitrate and chlorate, as a white pigment in paints or to preserve old frescoes. Hair dyes containing barium are also sold in the market in multiple countries [8–10], and barium sulfate ($BaSO_4$) is permitted by the EU, and may be used as a colorant in different cosmetics and personal care products. Furthermore, research on novel materials to be used in medical, industrial, and technological applications resulted in the development of nanoparticles (NPs) based on $BaSO_4$ [11, 12] or on barium composites [13, 14]; thus increasing the possibility of environmental contamination by barium [15, 16].

Inductively coupled plasma mass spectrometry (ICP–MS, in short), atomic absorption spectroscopy (AAS) and spectroscopic methods have been proposed previously to be used for the determination of barium concentration in different samples. However, these methods are not particularly suitable for on–site analysis, not easy to use, time-consuming, costly, and require experienced lab personnel and a well–equipped laboratory setting [17–20]. In contrast, potentiometric ion–selective electrodes (ISEs) have particular advantages including easy use, short response time, low limit of detection, wide concentration range, low cost, low–energy consumption, good selectivity and repeatability [21–23].

In the present study, we reported the development of novel Ba^{2+}–selective potentiometric sensors using new rhodanine derivative molecules as ionophores, tested their analytical performances, applied them to the analysis of barium in different water samples, and also studied their growth inhibitory potential against certain bacterial species.

ARTICLE IN PRESS

2. Experimental

2.1. Chemicals and Reagents

All reagents and solvents used in the synthesis of rhodanine derivative molecules were of high purity and were obtained from Sigma-Aldrich and Merck. To prepare potentiometric sensors, high molecular weight poly(vinyl chloride) (PVC, density, 1.4 g/mL at 25 °C, powder), bis (2–ethylhexyl) adipate (DEHA, density 0.925 g/mL at 20 °C), di-2-ethylhexyl) phthalate (DEHP, density 0.985 g/mL at 20 °C), dioctyl phenylphosphonate (DOPP, 0.967 g/mL at 25 °C), dibutyl phthalate (DBP) density 1.043 g/mL at 25 °C), *o*–nitrophenyloctylether (*o*–NPOE, density 1.04 g/mL at 25 °C), bis(2-ethylhexyl) sebacate (BEHS, density 0.914 g/mL at 25 °C), potassium tetrakis (*p*–chlorophenyl) borate (KT*p*ClPB, ≥98.0%) and tetrahydrofuran (THF, anhydrous, density, 0.889 g/mL at 25 °C) were purchased from Sigma Aldrich. All metal nitrate salts (Ba^{2+}, Na^{+}, Li^{+}, K^{+}, Ca^{2+}, Mg^{2+}, Pb^{2+}, Cu^{2+}, Zn^{2+}, Co^{2+}, Sr^{2+}, Mn^{2+}, Ni^{2+}, Cd^{2+}, Cr^{3+}, Al^{3+}, Gd^{3+}, Nd^{3+} and In^{3+}) used in selectivity studies were of analytical grade and were obtained from Sigma Aldrich, Fluka and Merck. Ultradistiled water (18.2 MΩ cm^{-1}; MP Minipure water system, Dest up, 0513957) was used to prepare stock solutions using metal nitrate salts. Sodium hydroxide pellets (NaOH), nitric acid (HNO_3) used in pH studies were purchased from Merck.

2.2. Apparatus

The ^{1}H–, ^{13}C–NMR and FT–IR instruments used in the characterization studies of the newly synthesized ionophores (**3** and **4**) are Bruker Avance DPX–400 spectrometer and Jasco FT/IR 430 instrument, respectively. The melting points of these molecules were determined by Electrothermal–9100 apparatus. Surface images and energy–dispersive X–ray (EDX) analysis of developed sensors were carried out with Quanta FEG 450–FEI instrument. Potentiometric measurements (Medisen Medical Company, Türkiye) were made using a two-electrode system with the prepared sensors and an Ag/AgCl reference electrode (Thermo Scientific Orion 900100).

ARTICLE IN PRESS

2.3. Method

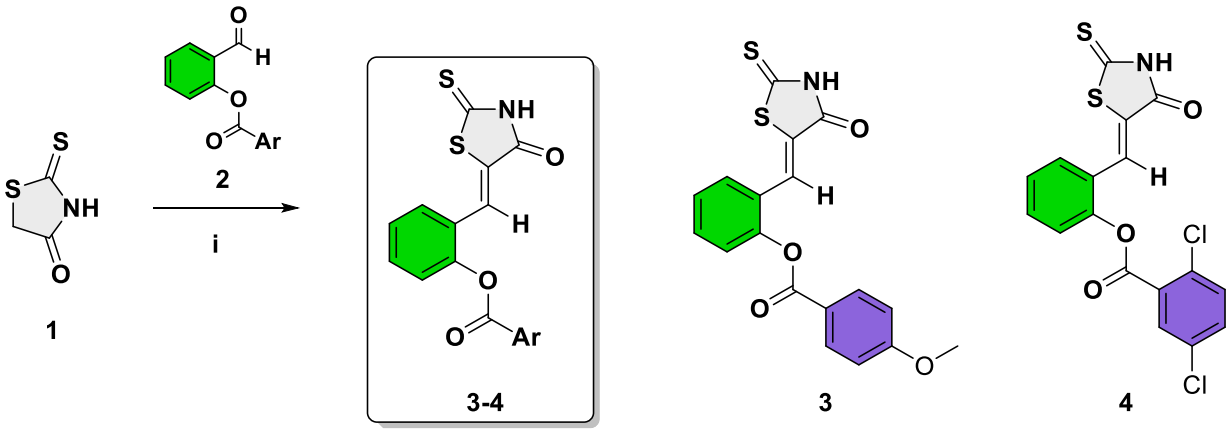
2.3.1. Synthesis of acyl aldehydes

The synthesis of acyl aldehydes was carried out as detailed in our previous study in the literature [24, 25]. Salicylaldehyde (1.22 g, 10 mmol) was dissolved in 50 mL of ethyl acetate and cooled in an ice bath. A solution containing the corresponding acyl chloride (10 mmol) and triethylamine (1.7 mL, 12 mmol) in 10 mL of ethyl acetate was added drop-wise under continuous stirring. After the addition was complete, the reaction mixture was allowed to warm to room temperature, and then stirred until complete conversion was confirmed by thin-layer chromatography (TLC). The reaction was quenched by the addition of 20 mL of water, and the aqueous layer was extracted with ethyl acetate (3×20 mL). The combined organic layers were dried over anhydrous sodium sulfate (Na_2SO_4), filtered, and concentrated under reduced pressure. The crude product was obtained as a white solid and used directly in the next step without further purification.

2.3.2. Synthesis of novel rhodanine derivatives

Rhodanine **1** (1.5 mmol, 200 mg) and the appropriate aldehyde **2** (1.0 mmol) were dissolved in 10 mL of ethanol in a 50 mL round-bottom flask. Piperidine (50 mol%, 0.5 mmol, 50 µL) was added as a catalyst, and the reaction mixture was refluxed for 5 hours. The progress of the reaction was monitored by thin-layer chromatography (TLC) using hexane/ethyl acetate (1:1, v/v) as the eluent. Upon completion, the temperature of the mixture was lowered down to room temperature, and the precipitated product was filtered, washed with cold ethanol and water, and dried under reduced pressure. The crude product was then recrystallized from ethanol to obtain the target compound in a good yield. ^{1}H–, ^{13}C– NMR, FT–IR and HRMS spectra of the synthesized molecules are presented in supplementary files (Figure S1–S8).

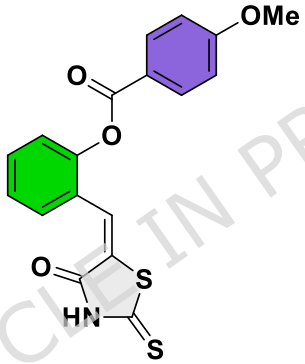
ARTICLE IN PRESS



i) Rhodanine (1.5 mmol), aldehyde **2** (1 mmol), piperidine (50% mol), EtOH, reflux, 5h.

Scheme 1. Synthesis of 5-Arylidenerhodanine derivatives via Knoevenagel condensation

(*E*)-2-((4-oxo-2-thioxothiazolidin-5-ylidene)methyl)phenyl 4-methoxybenzoate (3)

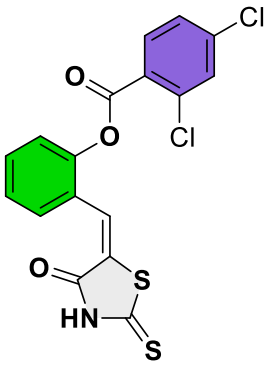


ARTICLE IN PRESS

Yellow solid, yield 74%, mp 240–244 ºC; R_f = 0.1 (EtOAc/hexanes = 7:3); ^{1}H NMR (400 MHz, DMSO–d_6) δ 13.86 (bs, 1H, NH), 8.12 (d, *J* = 8.8 Hz, 2H), 7.65–7.37 (m, 5H), 7.15 (d, *J* = 8.8 Hz, 2H), 3.87 (s, 3H). ^{13}C NMR (100 MHz, DMSO-d_6) δ 200.9 (C=S), 174.6 (C=O), 169.5 (C=O), 169.3 (Ar-C), 155.5 (Ar-C), 137.6 (Ar-2CH), 137.4 (CH=C), 134.0 (Ar-CH), 133.5 (Ar-CH), 132.5 (Ar-CH), 131.4 (Ar-C), 129.3 (Ar-C), 129.1 (Ar-CH), 125.4 (C=C), 119.9 (Ar-2CH), 61.1 (OMe). FTIR (cm^{-1}) 3095, 2974, 2844, 1723, 1703, 1595, 1199, 1162, 835. HRMS (QTOF, ESI+) m/z: $[M + Na]^+$ calc for $C_{18}H_{13}NO_4S_2Na$, 394.0184; found 394.0179.

ARTICLE IN PRESS

(*E*)-2-((4-oxo-2-thioxothiazolidin-5-ylidene)methyl)phenyl 2,4-dichlorobenzoate (4)



Yellow solid, yield 78%, mp 245–249 ^{o}C; R_f = 0.2 (EtOAc/hexanes = 7:3); ^{1}H NMR (400 MHz, DMSO-d_6) δ 13.90 (bs, 1H, NH), 8.20 (d, *J* = 8.5 Hz, 1H), 7.93 (d, *J* = 1.9 Hz, 1H), 7.71 (dd, *J* = 8.5, 1.9 Hz, 1H), 7.64-7.54 (m, 5H). ^{13}C NMR (100 MHz, DMSO–d_6) δ 196.4 (C=S), 170.3 (C=O), 163.0 (C=O), 149.9 (Ar-C), 139.0 (C=CH), 134.5 (Ar–C), 133.8 (Ar–CH), 132.4 (Ar–C), 131.3 (Ar–C), 129.5 (Ar–CH), 129.2 (Ar–CH), 128.5 (Ar–CH), 128.0 (Ar–CH), 127.5 (Ar–CH), 126.5 (Ar–C), 124.1 (Ar–CH), 123.9 (C=C). FTIR (cm^{-1}) 3143, 3042, 2845, 1748, 1692, 1582, 1209. HRMS (QTOF, ESI+) m/z: $[M + Na]^+$ calc for $C_{17}H_9Cl_2NO_3S_2Na$, 431.9299; found 431.9293

2.3.3. Preparation of rhodanine based sensors

In the current study, solid contact PVC membrane sensors were developed in two steps as detailed in our previous studies [26, 27]. First, the solid contact electrodes were prepared by dissolving graphite (50.0%), epoxy (35.0%) and hardener (15.0%) in approximately 3 mL of THF, and mixing until a certain viscosity was reached. Then, copper wires with one open end, approximately 15 cm in length, were dipped into this mixture several times, and then the coated copper wires were left to dry for 24h at room conditions. Then, polymer membrane sensors were prepared, in which two different rhodanine derivative molecules (**3** and **4**) were used as ionophores. For this purpose, ionophore, plasticizer, lipophilic additive (KT*p*ClPB) and PVC were dissolved in approximately 3 mL of THF in the proportions given in Table 1 and mixed until a certain viscosity was obtained. The previously prepared solid contact electrodes were dipped into the PVC membrane mixture several times, and their surfaces were coated. The coated electrodes were left to dry for 12h at room conditions. The potentiometric performance

ARTICLE IN PRESS

properties of the sensors prepared in the ratios in Table 1 were tested in laboratory conditions, and the performance properties of the sensors with optimum working conditions where these molecules (**3** and **4**) were used as ionophores were examined in further detail. Potential readings were systematically recorded using an Ag/AgCl reference electrode, ensuring a stable and reproducible reference point for all measurements. The temperature was rigorously maintained at a constant 25 ± 1.0 °C throughout the experiments to minimize thermal fluctuations that could affect electrochemical responses. The electrochemical cell configuration employed for these measurements was meticulously set up as follows:

Ag/AgCl; KCl (3M) ‖Ba^{2+} sample solution │ Ba^{2+} selective membrane │solid contact │Cu wire

This configuration allowed for precise measurement of the potential difference generated by the interaction between the Ba^{2+} ions and the selective sensor membrane, relative to the stable Ag/AgCl reference electrode. All potential measurements were performed in triplicate.

ARTICLE IN PRESS

For potentiometric measurements, the relationship between concentration and potential is governed by the Nernst equation, where *E* represents the cell potential observed at zero current.

$$E = E^{o} + \frac{RT}{nF} In[a_i]$$

Here, *E* is the potential (V), *E*° is the standard potential, n is the number of electrons, and *a*i is the activity of the primary ion. *R*, *T*, and *F* are known constants. The sensitivity of a potentiometric sensor is known to be limited to 59.2/z mV at room temperature, the slope predicted from the Nernst equation, where z is the charge of the analyte ion. The potentiometric response of the Ba^{2+}–selective electrode was described by the Nernst equation:

$$E = E^{o} + \frac{0.05916}{z} \log[Ba^{2+}]$$

Since the analyte charge is 2 (z = 2), the mathematical relationship between the measured potential (mV) and the analyte concentration is:

ARTICLE IN PRESS

$$E = E^{o} + 0.02958\log[Ba^{2+}]$$

2.3.4. Disk diffusion method for the analysis of bacterial growth inhibitory potentials of novel molecules

To examine the growth inhibitory potential of the newly synthesized rhodanine derivative molecules against six different selected bacterial species, a disk diffusion microbial susceptibility test using these new molecules was performed according to the procedure used in our previous study [21].

3. Results and Discussion

3.1. Characterization of novel rhodanine derivatives

As part of the present study, two novel 5-arylidene rhodanine derivatives were successfully synthesized. Following the synthesis protocol outlined in Scheme 1, the target compounds **3** and **4** were obtained via a piperidine-catalyzed Knoevenagel condensation between rhodanine and the corresponding aldehyde derivatives designed for this work. The reactions proceeded smoothly, producing the desired molecules in satisfactory yields. ^{1}H NMR analysis of compound **3** revealed a characteristic broad singlet at δ 13.86 ppm, corresponding to the NH proton of the rhodanine moiety. Aromatic and vinylic protons were observed in the region of δ 8.20–7.15 ppm, exhibiting splitting patterns consistent with their respective chemical environments and proton counts. In addition, the methoxy protons in compound **3** appeared as a singlet at δ 3.87 ppm. In the ^{13}C NMR spectra, the C=S carbon of the rhodanine ring resonated at δ 200.9 ppm in compound **3;** while in compound **4,** it appeared slightly upfield at δ 196.4 ppm. The carbonyl (C=O) signals were observed in the range of δ 174.6–163.0 ppm. Vinyl and aromatic carbons gave resonances between *δ* 169.3 and 119.9 ppm, consistent with the expected number of carbon atoms. Additionally, the methoxy carbon in compound **4** appeared in the aliphatic region at δ 61.1 ppm. FT–IR spectral analysis further supported the structural assignments. The N–H stretching vibrations were observed between 3095 and 3143 cm^{-1}.

ARTICLE IN PRESS

Aromatic C–H stretching bands appeared in the range of 2974–3042 cm^{-1}, while aliphatic C–H stretching bands were detected at 2844–2845 cm^{-1}. The ester C=O stretching vibrations were observed between 1723 and 1748 cm^{-1} in both compounds, whereas the C=O stretching bands of the rhodanine moiety appeared at 1692–1703 cm^{-1}. Conjugated C=C stretching vibrations were also recorded in the range of 1592–1595 cm^{-1}.

3.2. Membrane composition

In the current study, two newly synthesized rhodanine-derived molecules were utilized as ionophores, and 16 sensors with different compositions were prepared in total. The synthesized rhodanine derivatives exhibited selectivity towards Ba^{2+} ions over different cationic species.

Ion-selective sensors are analytical systems that can identify a specific ion (analyte) with high selectivity in a complex medium. This selectivity is achieved thanks to molecules called ionophores located in the active phase of the sensor. The ionophore has the ability to reversibly and selectively complex with the target ion and carries it to the membrane phase, thus enabling the ion to pass into the membrane; this ion distribution creates a phase-boundary potential at the membrane surface. In potentiometric measurement, the potential difference between the reference electrode and the ion-selective electrode originates from this phase-boundary potential and is directly dependent on the analyte ion activity.

The enhanced sensing performance of molecule **4** relative to molecule **3** can be attributed to the electron-withdrawing 2,4-dichloro substituents, which increase the polarization of the rhodanine-ester framework and strengthen interactions with Ba^{2+} ions. In contrast, the electron-donating methoxy group in molecule **3** reduces binding efficiency, leading to lower sensitivity.

ARTICLE IN PRESS

These electronic effects provide a clear structure–performance relationship for the observed sensor behavior.

The compositions and potentiometric performance properties of the prepared sensors are given in Table 1. The detection limit values given in Table 1 were calculated by substituting the potential value corresponding to the point where the horizontal and vertical axes of the calibration curves intersect in the linear equation according to the rules stated by IUPAC [28]. Among the sensors with the same composition, the sensor prepared with molecule **4** (sensor 10) was found to have a broader concentration range and lower detection limit than the sensor prepared with molecule **3** (sensor 2). The behavior of the electrodes that do not contain the synthesized rhodanine derivatives (**3** and **4**) in their composition against Ba^{2+} ions is given in Figure 1. As shown in this Figure, the sensors not having the synthesized rhodanine derivatives in their composition in the concentration range of 1.0×10^{-5}–1.0×10^{-1} M fail to exhibit a significant potential response.

ARTICLE IN PRESS

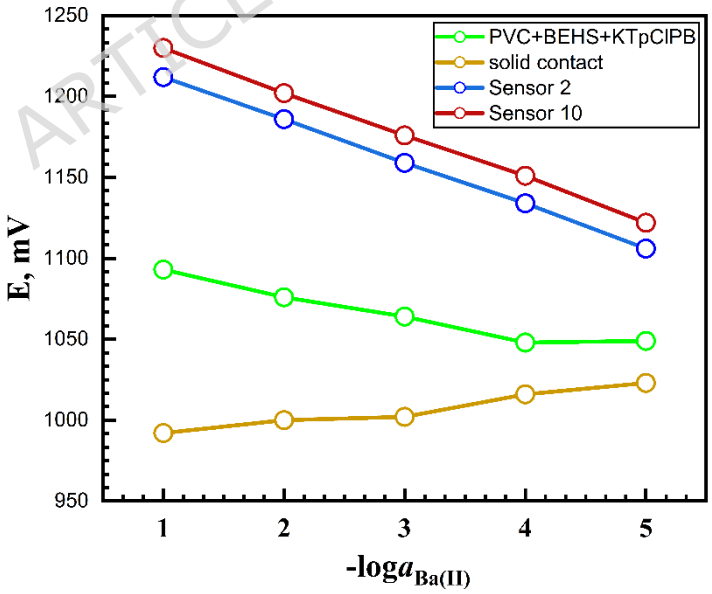
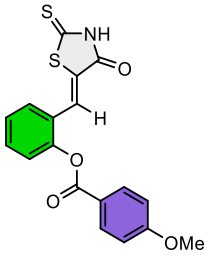
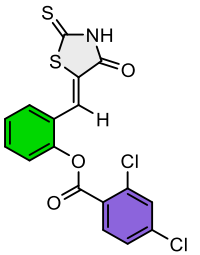


Figure 1. Effect of synthesized rhodanine derivatives on the sensor behavior.

Table 1. PVC membrane potentiometric sensors prepared with newly synthesized rhodanine derivatives in this study, and their certain potentiometric performance properties.

Sensor No	Ionophore	Membrane composition (*w*/*w*)									Potentiometric performance			
		Ionophore	PVC	Plasticizers						KT*p*ClPB	Linear range, M	Detection limit, M	Slope (mV/decade)	R^2
				DEHA	BEHS	DBP	DOPP	*o*–NPOE	DEHP					
1	 **3**	32.0	3.0	64.0						1.0	1.0×10^{-5}–1.0×10^{-1}	7.40×10^{-6}	19.5 ± 0.8	0.9982
2		**32.0**	**3.0**		**64.0**					**1.0**	**1.0×10^{-6}–1.0×10^{-1}**	**7.66×10^{-7}**	**25.0 ± 2.5**	**0.9972**
3		32.0	3.0			64.0				1.0	1.0×10^{-5}–1.0×10^{-3}	9.24×10^{-6}	14.5 ± 4.5	0.9689
4		32.0	3.0				64.0			1.0	1.0×10^{-3}–1.0×10^{-1}	2.40×10^{-4}	25.1± 2.0	0.9612
5		32.0	3.0					64.0		1.0	1.0×10^{-5}–1.0×10^{-1}	9.79×10^{-6}	22.0 ± 2.1	0.9963
6		32.0	3.0						64.0	1.0	1.0×10^{-5}–1.0×10^{-1}	9.43×10^{-6}	23.8 ± 3.6	0.9912
7		32.0	2.0		65.0					1.0	1.0×10^{-5}–1.0×10^{-1}	8.99×10^{-6}	19.0 ± 4.9	0.9771
8		32.0	4.0		63.0					1.0	1.0×10^{-5}–1.0×10^{-1}	8.89×10^{-6}	20.6 ± 2.9	0.9918
9	 **4**	32.0	3.0	64.0						1.0	1.0×10^{-5}–1.0×10^{-1}	8.91×10^{-6}	19.2 ± 3.3	0.9953
10		**32.0**	**3.0**		**64.0**					**1.0**	**1.0×10^{-7}–1.0×10^{-1}**	**9.77×10^{-8}**	**27.0 ± 2.3**	**0.9977**
11		32.0	3.0			64.0				1.0	1.0×10^{-5}–1.0×10^{-1}	6.98×10^{-6}	20.5 ± 3.4	0.9943
12		32.0	3.0				64.0			1.0	1.0×10^{-4}–1.0×10^{-1}	2.41×10^{-5}	20.0 ± 4.0	0.9869
13		32.0	3.0					64.0		1.0	1.0×10^{-5}–1.0×10^{-1}	9.66×10^{-5}	14.3 ± 2.0	0.9871
14		32.0	3.0						64.0	1.0	1.0×10^{-4}–1.0×10^{-1}	2.0×10^{-5}	29.6 ± 2.8	0.9819
15		32.0	2.0		65.0					1.0	1.0×10^{-5}–1.0×10^{-1}	9.40×10^{-6}	24.3 ± 4.1	0.9905
16		32.0	4.0		63.0					1.0	1.0×10^{-5}–1.0×10^{-1}	7.86×10^{-6}	25.5 ± 1.1	0.9953

ARTICLE IN PRESS

3.3. Potentiometric response and calibration curve

The potential responses and calibration curves of the sensors prepared using newly synthesized rhodanine-derived molecules as ionophores are given in Figure 2 (a–d). According to Figure 2, the sensor 10 prepared with molecule 4 has a linear working range of 1.0×10^{-7}–1.0×10^{-1} M (R^2 = 0.9977) and a detection limit of 9.77×10^{-8} M, while the sensor 2 prepared with molecule 3 has a linear working range of 1.0×10^{-6} –1.0×10^{-1} M (R^2 = 0.9972) and a detection limit of 7.66×10^{-7} M. Sensor 2 has a near–Nernstian response of 25.0±2.5 mV/decade, whereas sensor 10 has a Nernstian response of 27.0±2.3 mV/decade. As a result, sensor 10 prepared using molecule 4 as ionophore has optimum composition (3.0% ionophore (**4**), 32.0% PVC, 64.0%BEHS and 1.0% KT*p*ClPB) and is selective towards Ba^{2+} ions.

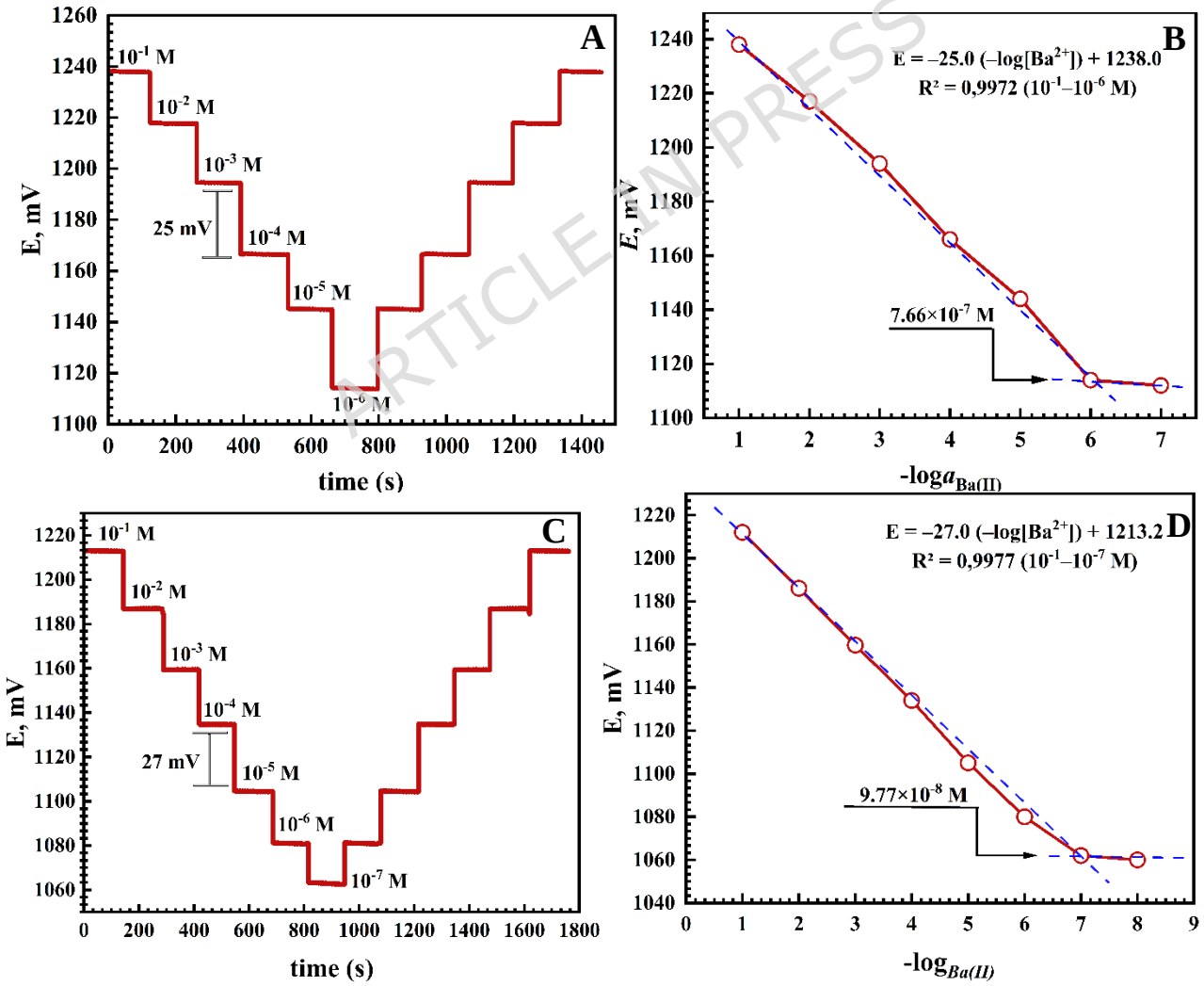


Figure 2 a–b) Potentiometric response and calibration curve of sensor 2 **c–d)** Potentiometric response and calibration curve of sensor 10.

ARTICLE IN PRESS

3.4. Repeatability

The repeatability of a sensor is a crucial indicator of its precision and reliability in providing consistent measurements under identical conditions. To rigorously assess this, the optimized rhodanine-based potentiometric sensor was subjected to repeated measurements of Ba^{2+} solutions at three different concentrations: 10^{-2}, 10^{-3} and 10^{-4} M. These concentrations represent the higher and middle range of the sensor's linear detection capability, providing a comprehensive evaluation of its performance. The repeatability plot and repeatability data of sensors 2 and 10 prepared with molecules **3** and **4**, respectively, are given in Figure 3a–b and Table 2. When these data was analysed, the sensors prepared with the optimum components exhibited a repeatable behavior in the studied concentration range (10^{-2}, 10^{-3} and 10^{-4} M). According to Table 2, the prepared optimum sensor 2 was found to have lower standard deviations than sensor 10 at three different concentrations, respectively, of ±1.32, ±0.34, and ±1.13.

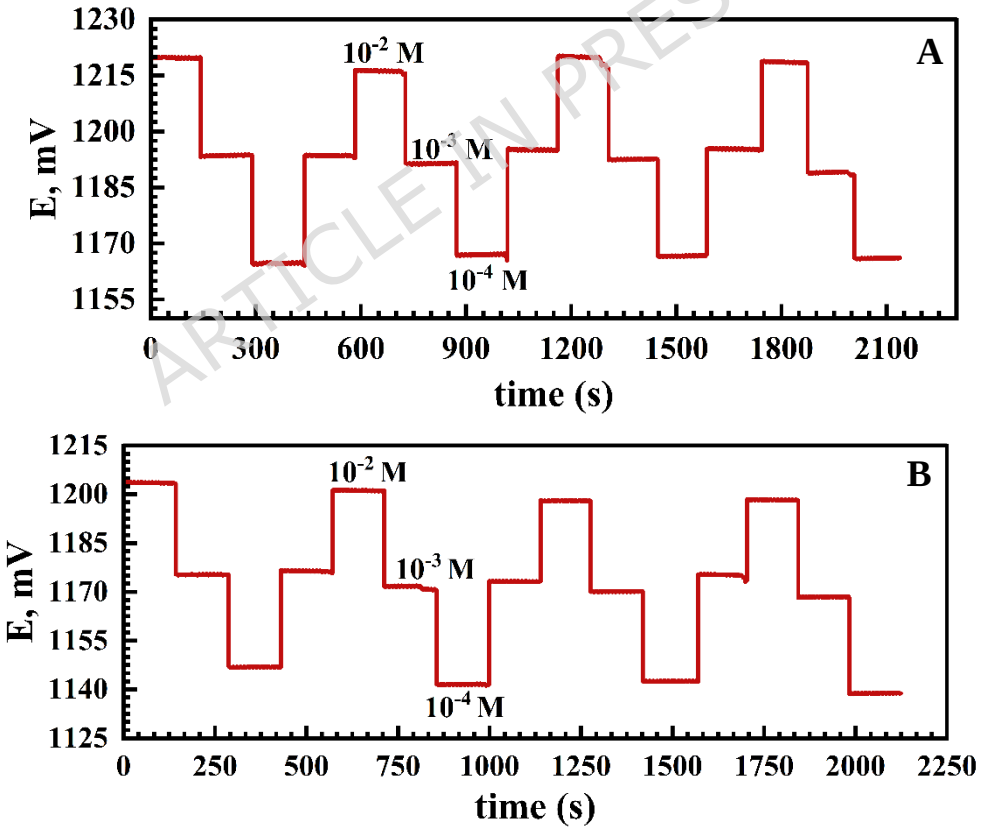


Figure 3 a–b) Repeatability analysis of sensors 2 and 10 against Ba^{2+} solutions of different concentrations.

ARTICLE IN PRESS

Table 2. Repeatability data of sensors 2 and 10 against Ba^{2+} solutions with different concentrations.

Sensor	Concentration, M	Potentials, mV			
		I	II	III	Average (±SD)
2	1.0×10^{-2}	1216.75	1219.94	1218.75	1218.48 (±1.32)
	1.0×10^{-3}	1193.56	1193.50	1192.81	1193.29 (±0.34)
	1.0×10^{-4}	1164.38	1166.81	1166.75	1165.89 (±1.13)
10	1.0×10^{-2}	1201.19	1198.19	1198.5	1199.29 (±1.35)
	1.0×10^{-3}	1171.69	1170.19	1168.5	1170.12 (±1.30)
	1.0×10^{-4}	1141.69	1142.56	1138.69	1140.98 (±1.65)

3.5. Potentiometric selectivity

Selectivity, which is undoubtedly one of the most important potentiometric performance properties of ion-selective sensors, is extremely critical in terms of determining the ionic species to which the prepared sensor is selective against different species. ISEs can of course respond to other species present in the environment; but, they should be selective against only one species. The selectivity values of the sensors which were prepared with molecules 3 and 4 is given in Figure 4 (a–b) which shows that the sensors prepared with the newly synthesized rhodanine derivative molecules exhibited very high selectivity against Ba^{2+} ions. The numerical expression of how well an ISE can differentiate the analyte ion from other interfering ions is determined with the help of selectivity coefficients. In the current study, the selectivity coefficients of the proposed sensor were calculated with the separate solution method of IUPAC [29]. The calculated selectivity coefficient values are shown in Table 3. When the data given in Figure 4 and Table 3 are analyzed, it is clearly observed that the prepared sensors show high selectivity to Ba^{2+} ions.

ARTICLE IN PRESS

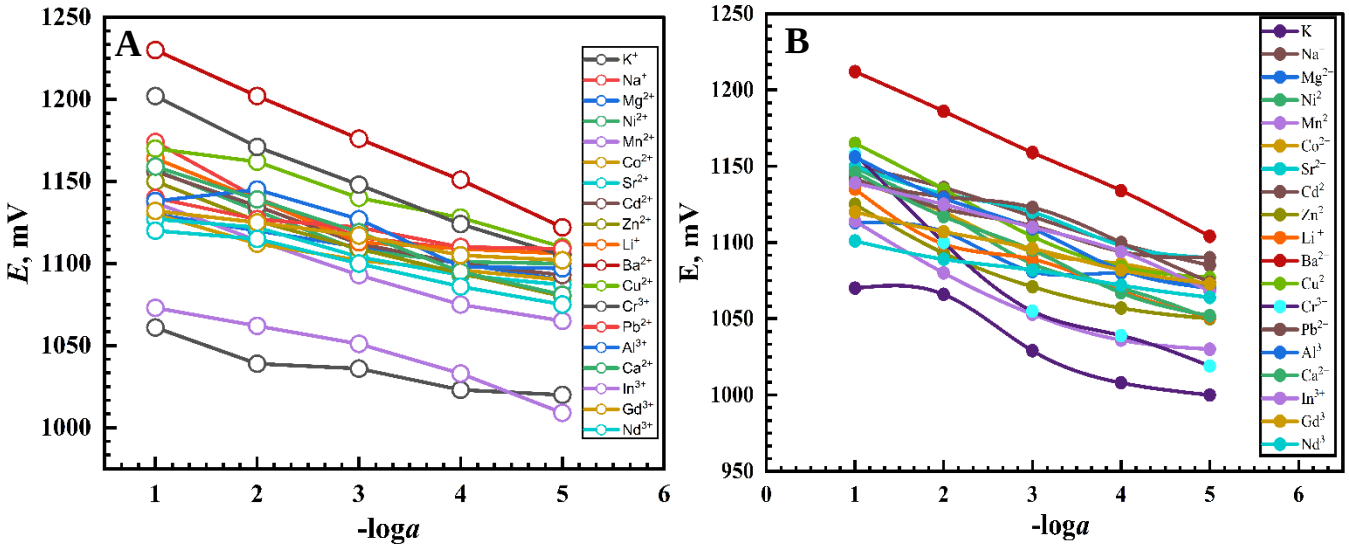


Figure 4. Potentiometric selectivity of sensors developed with newly synthesized rhodanine derivatives **a)** Sensor 2 **b)** Sensor 10.

Table 3. Potentiometric selectivity of sensors 2 and 10 calculated according to IUPAC rules.

Sensor 2			**Sensor 10**		
Interfering ions	$logK^{pot}_{Ba(II),M^{n+}}$	$K^{pot}_{Ba(II),M^{n+}}$	Interfering ions	$logK^{pot}_{Ba(II),M^{n+}}$	$K^{pot}_{Ba(II),M^{n+}}$
Cr^{+3}	–1.05	8.91×10^{-2}	Na^{+}	–1.69	2.04×10^{-2}
Cu^{2+}	–1.35	4.47×10^{-2}	Cu^{2+}	–1.72	1.91×10^{-2}
Al^{3+}	–1.93	1.17×10^{-2}	Sr^{2+}	–1.83	1.45×10^{-2}
Na^{+}	–2.09	8.13×10^{-3}	Pb^{2+}	–1.89	1.29×10^{-2}
Li^{+}	–2.13	7.41×10^{-3}	Al^{3+}	–1.93	1.17×10^{-2}
Ca^{2+}	–2.14	7.24×10^{-3}	In^{3+}	–2.06	8.71×10^{-3}
Cd^{2+}	–2.26	5.49×10^{-3}	Cd^{2+}	–2.16	6.92×10^{-3}
Ni^{2+}	–2.36	4.36×10^{-3}	Ni^{2+}	–2.23	5.89×10^{-3}
Pb^{2+}	–2.54	2.88×10^{-3}	Co^{2+}	–2.24	5.75×10^{-3}
Zn^{2+}	–2.57	2.69×10^{-3}	Ca^{2+}	–2.33	4.68×10^{-3}
Gd^{3+}	–2.60	2.51×10^{-3}	Gd^{3+}	–2.67	2.14×10^{-3}
Sr^{2+}	–2.70	1.99×10^{-3}	Mg^{2+}	–2.68	2.09×10^{-3}
Mg^{2+}	–2.77	1.70×10^{-3}	Cr^{+3}	–2.91	1.23×10^{-3}
Nd^{3+}	–2.94	1.15×10^{-3}	Li^{+}	–2.94	1.15×10^{-3}
Mn^{2+}	–2.97	1.07×10^{-3}	Zn^{2+}	–3.14	7.24×10^{-4}
Co^{2+}	–3.04	9.12×10^{-4}	Nd^{3+}	–3.28	5.25×10^{-4}
In^{3+}	–4.74	1.82×10^{-5}	Mn^{2+}	–3.58	2.63×10^{-4}
K^{+}	–5.51	3.10×10^{-6}	K^{+}	–4.05	8.91×10^{-5}

ARTICLE IN PRESS

ARTICLE IN PRESS

3.6. Response time

Next, the response time of the prepared Ba^{2+}–selective sensors was determined by considering the rules of IUPAC [28]. IUPAC defines the response time as 95% of the time required for the electrode to reach equilibrium for each 10–fold concentration change and is shown as t_{95}. For this purpose, the equilibrium times of the sensors during the transition from one concentration to another were determined. Based on data given in Figure 5a–b, the response times of sensor 2 and sensor 10 were determined as 6 and 5 s, respectively.

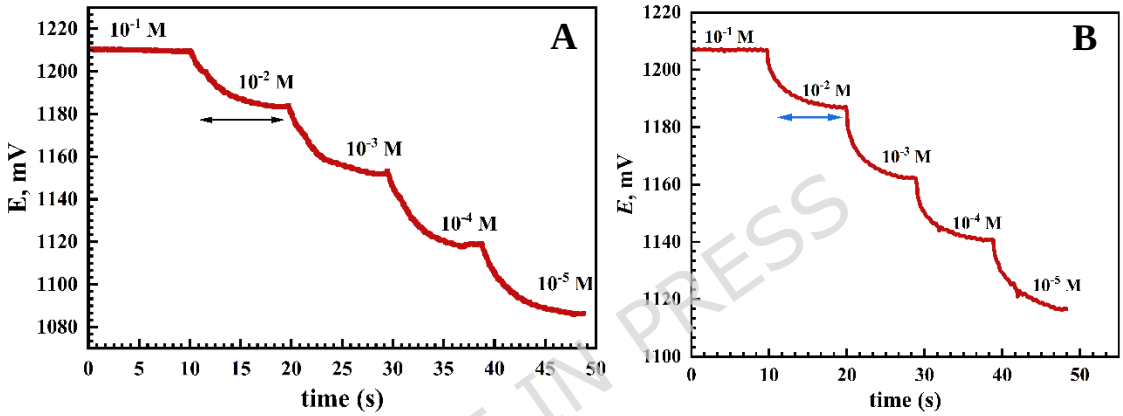


Figure 5 a–b) Response time of sensors 2 and 10, respectively.

3.7. pH range

The pH ranges in which rhodanine-based sensors can work without being influenced by the changes in pH were determined using acid–base solutions prepared in the pH range of 2.0–12.0. The acidic pH (2.0–7.0) solution was prepared using HNO_3, the basic pH (8.0–12.0) solution was prepared using NaOH, and two different concentrations (10^{-2} and 10^{-3} M) of Ba^{2+} ion solutions were added to these solutions. The potential changes of both sensors for two different concentrations in the pH 2.0–12.0 range were then examined. The potential–pH graph was drawn with the obtained data to determine the pH working ranges of the sensors (Figure 6a–b). According to Figure 6a–b, sensor 2 prepared with molecule **3** was observed to be able to work without being influenced by changes in pH in the range of pH 5.0–8.0 in both concentrations, while sensor 10 prepared with molecule **4** could work without being affected by pH changes in

ARTICLE IN PRESS

the range of pH 5.0–9.0 in both concentrations. For prepared two sensors, the high potential values below this pH working range may be due to the presence of hydronium ions, while the low potential values above this range may be observed because $Ba(OH)_2$ complexes form.

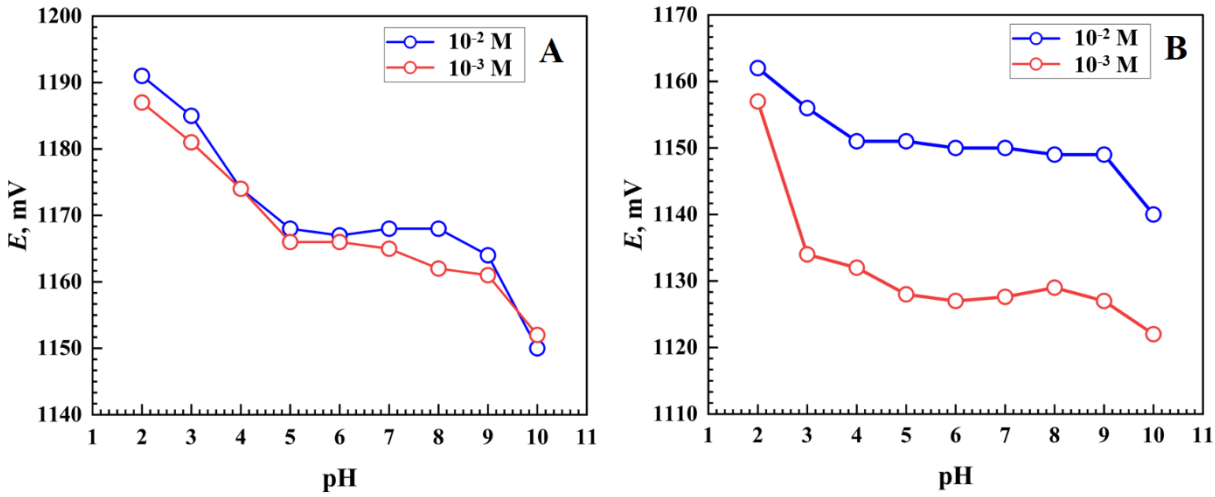
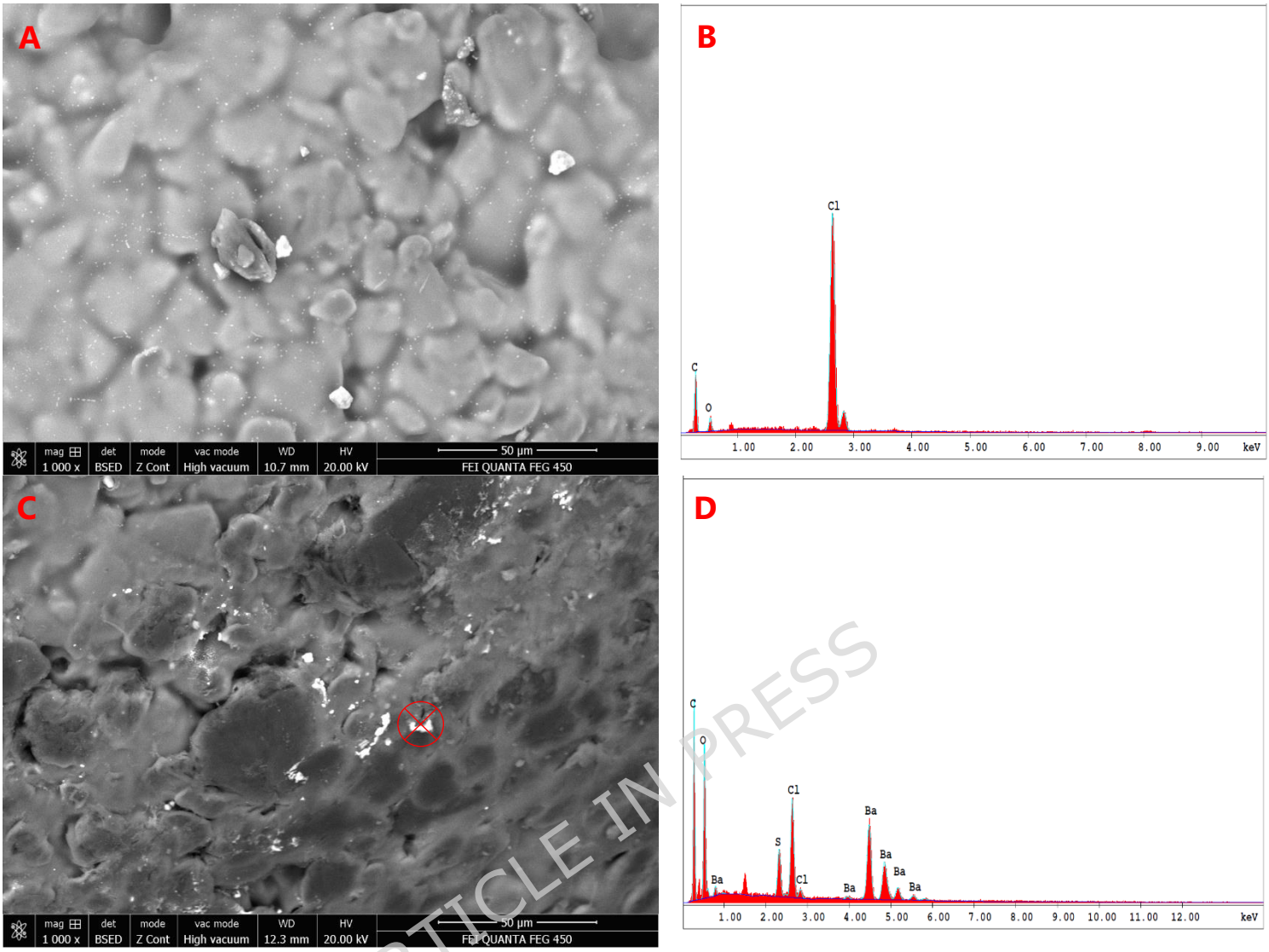


Figure 6. pH working range of **a-)** sensors 2 and **b-)** sensor 10 at two different concentrations.

3.8. Surface morphologies of the prepared sensors

Later in the study, the surfaces of the sensors with optimum composition prepared with two different rhodanine derivatives synthesized were studied using scanning electron microscopy. Before this analysis, some sensors were conditioned in 10^{-2} M ion solutions for 30 minutes. Surface images and EDX spectra of conditioned and unconditioned sensors are given in Figures 7 and 8 for sensors 2 and 10, respectively. While only PVC membrane components are present in the EDX spectrum of unconditioned sensors, the presence of barium ions is remarkable in the EDX spectrum of conditioned sensors. The white dots in the SEM images belong to Ba^{2+} ions, and it is clearly observed in the EDX spectrum of Figures 7d and 8d that Ba^{2+} ions are attached to the sensor surface. Combined, based on the data from SEM/EDX analysis, it can be said that Ba^{2+} ions can be attached to the cavities on the surface of the sensors, and the sensor can detect Ba^{2+} ions.



ARTICLE IN PRESS

Figure 7. Sensor 2 in Ba^{2+} ion solution: **a)** Unconditioned surface image **b)** EDX spectrum of the unconditioned surface **c)** Conditioned surface image after 30 minutes **d)** EDX spectrum of the conditioned surface.

ARTICLE IN PRESS

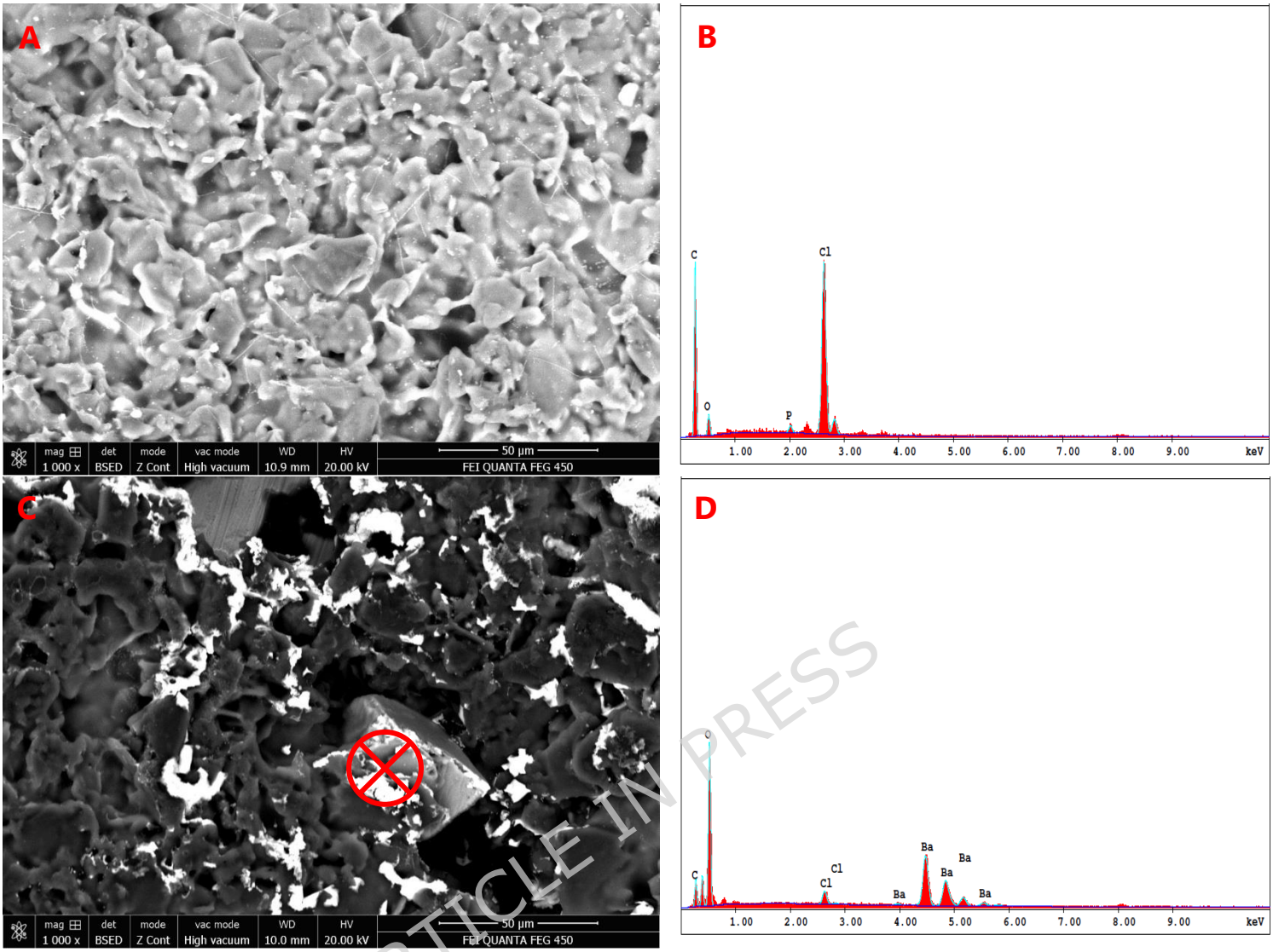


Figure 8. Sensor 10 in Ba^{2+} ion solution: **a)** Unconditioned surface image **b)** EDX spectrum of the unconditioned surface **c)** Conditioned surface image after 30 minutes **d)** EDX spectrum of the conditioned surface.

3.9. Analytical applications

In this study, when all the obtained data are evaluated, it is clearly seen that sensor 10 has better potentiometric performance compared to sensor 2. Therefore, Ba^{2+} ion concentrations in five different water samples were determined only using sensor 10. All water samples were collected in clean bottles, immediately stored at 4 °C, and analyzed within 24 hours of collection to avoid any contamination or changes in ion concentration.

ARTICLE IN PRESS

Ba^{2+} ions were added to the water samples at the rates given in Table 4, and subsequently potentiometric measurements were taken with the prepared sensor. The potential values obtained were then written in the calibration curve, and the Ba^{2+} ion concentration in each sample was calculated. According to the obtained data, the produced sensor can be proposed to be able to determine Ba^{2+} ions at high recovery rates (>97.98).

Table 4. Applications of the Ba^{2+}–selective sensor in real samples.

Real Samples	**Added Ba^{2+} (ppm)**	**Found Ba^{2+} concentration, ppm***	**%Recovery**
Purified water	56.0	54.87 (±0.14)	97.98
Tap water (Tokat, Turkey)		55.31 (±0.57)	98.77
Spring water		55.46 (±0.57)	99.04
Snow water		55.56 (±0.40)	98.78
Bottled water		55.57 (±0.21)	98.52

*Average value (n = 3).

ARTICLE IN PRESS

3.10. Comparison study

The sensors reported in the present study were compared with other sensors previously reported in the literature with respect to linear working range, detection limit, Nernstian response, pH working range and response time (Table 5). Based on the data given in Table 5, fabricated sensor 10 was found to have the widest linear working range, the lowest detection limit and the fastest response time relative to its counterparts in the literature. The data we obtained show that the synthesized new molecule **4** exhibits a very successful performance in the determination of Ba^{2+} ions when compared to other studies in the literature.

ARTICLE IN PRESS

Table 5. Comparation of the prepared sensor to the other reported Ba^{2+}–selective potentiometric sensors.

Ionophore	Linear range, M	Limit of detection, M	Slope, mV dec^{-1}	pH working range	Response time, s	Ref.
Thiosemicarbazone derivative molecule	1.0×10^{-6} – 1.0×10^{-1}	5.54×10^{-7}	28.9±1.43	6.0–9.0	<10	[30]
Dimethyl-4,4-dimethoxy-5,6,5,6-dimethylene dioxy biphenyl-2,2-dicarboxylate	1.0×10^{-5} – 1.0×10^{-1}	5.0×10^{-6}	Not reported	4.0–9.0	Not reported	[31]
2,3,4-pyridine-1,3,5,7,12-pentaazacyclopentadeca-3-ene	1.41×10^{-6} – 1.0×10^{-1}	Not reported	30.0	2.5–7.0	18	[32]
4-4'-methylenediantipyrine	1.0×10^{-6} – 1.0×10^{-2}	5.2×10^{-7}	29.7±0.3	3.4–10.6	15	[33]
Barium(II)–Rose Bengal	5.0×10^{-5} – 1.0×10^{-1}	2.5×10^{-6}	28.5±0.4	4.5–10.0	20	[34]
3-deoxy-D-erythro-hexos-2-ulose bis (thiosemicarbazone)	1.0×10^{-6} – 1.0×10^{-2}	5.6×10^{-7}	29.6±0.5	2.6–11.0	15	[35]
4-aminobenzoic acid 2-diethylaminoethyl ester	1.0×10^{-5} – 1.0×10^{-1}	4.23×10^{-6}	Not reported	5.0–11.0	8	[36]
Dibenzo-24-crown-8	1.0×10^{-6} – 1.0×10^{-3}	6.1×10^{-7}	30.1	4.1–9.0	<10	[37]
1,2-bis(diarylphosphine oxide) naphthalene	1.0×10^{-5} – 1.0×10^{-1}	5.0×10^{-6}	30.0	3.0–11.0	60	[38]
macrocyclic tetrabasic ligand	3.6×10^{-6} – 1.0×10^{-1}	1.9×10^{-6}	29.7±0.2	2.5–7.5	10	[39]
(*E*)-2-((4-oxo-2-thioxothiazolidin-5-ylidene)methyl)phenyl 4-methoxybenzoate **(3)**	1.0×10^{-6} – 1.0×10^{-1}	7.66×10^{-7}	25.0±2.5	5.0–8.0	6	This work
(*E*)-2-((4-oxo-2-thioxothiazolidin-5-ylidene)methyl)phenyl 2,4-dichlorobenzoate **(4)**	1.0×10^{-7} – 1.0×10^{-1}	9.77×10^{-8}	27.0±2.3	5.0–9.0	5	

ARTICLE IN PRESS

3.11. Growth inhibitory potential of the novel molecules against certain bacterial species-specific

The antimicrobial test results of the synthesized molecules are interpreted in detail in the supplementary files.

4. Conclusion

In the current study, two new molecules derived from rhodanine were synthesized for the first time, and their sensor properties and certain biological activities were analyzed. A total of 16 sensors with different compositions were prepared, and the potentiometric performance characteristics of the sensors prepared with two different molecules providing optimum

ARTICLE IN PRESS

conditions were compared with each other. Sensor 10 prepared with molecule 4 showed better performance than sensor 2 prepared with molecule 3 in terms of particular performance properties such as working range, detection limit, response time and pH working range. The obtained results indicate that both synthesized rhodanine derivative molecules can be used as ionophores in the potentiometric analysis of Ba^{2+} ions; however, molecule 4 shows better sensor properties. These molecules were also found to have growth inhibitory potentials depending on bacterial species.

Declarations

Abbreviations

SEM: Scanning electron microscope

EDX: Surface images and energy–dispersive X–ray

FTIR: Fourier Transform Infrared Spectroscopy

NMR: Nuclear magnetic resonance

Q-TOF (HRMS): Quadrupole Time-of-Flight mass spectrometry

ISEs: Ion selective electrodes

PVC: Poly(vinyl chloride)

DEHA: Bis (2–ethylhexyl) adipate

DEHP: Di-2-ethylhexyl) phthalate

DOPP: Dioctyl phenylphosphonate

DBP: Dibutyl phthalate

BEHS: Bis(2-ethylhexyl) sebacate

o–NPOE: *o*–nitrophenyloctylether

KT*p*ClPB: Potassium tetrakis (*p*–chlorophenyl) borate

THF: Tetrahydrofuran

NaOH: Sodium hydroxide

HNO_3: Nitric acid

IUPAC: International Union of Pure and Applied Chemistry

Ethics approval and consent to participate

Not applicable

ARTICLE IN PRESS

Consent for publication

Not applicable

Availability of data and materials

Not applicable.

Competing Interests

The authors of the present study declare no conflict of interest.

Funding

The authors thank the The Scientific and Technological Research Council of Turkey (TUBITAK) (Project Number: 124Z600) for its support. Onur Cem Altunoluk was supported financially by TUBITAK–BIDEB 2210/A Scholarship Program for M.Sc. students.

Authors' contributions

Onur Cem Altunoluk: Investigation, Analysis, **Oguz Ozbek:** Investigation, Analysis, Writing - Review&Editing, **Erbay Kalay:** Investigation, Analysis, Writing - Review&Editing, **Caglar Berkel:** Investigation, Analysis, Writing - Review&Editing, **Ömer Isildak:** Investigation, Analysis.

ARTICLE IN PRESS

Acknowledgements

Not applicable.

References

[1] M. Peana, S. Medici, M. Dadar, M.A. Zoroddu, A. Pelucelli, C.T. Chasapis, G. Bjørklund, Environmental barium: potential exposure and health-hazards, Arch Toxicol, 95 (2021) 2605-2612. https://doi.org/10.1007/s00204-021-03049-5

[2] M.A. Zoroddu, S. Medici, A. Ledda, V.M. Nurchi, J.I. Lachowicz, M. Peana, Toxicity of nanoparticles, Curr Med Chem, 21 (2014) 3837–3853. https://doi.org/10.2174/09298673216661406011623 14

ARTICLE IN PRESS

[3] M.R. Krejci, B. Wasserman, L. Finney, I. McNulty, D. Legnini, S. Vogt, D. Joester, Selectivity in biomineralization of barium and strontium, J Struct Biol, 176 (2011) 192–202. https://doi.org/10.1016/j.jsb.2011.08.006

[4] D. Poddalgoda, K. Macey, H. Assad, K. Krishnan, Development of biomonitoring equivalents for barium in urine and plasma for interpreting human biomonitoring data. Regul Toxicol Pharmacol 86 (2017) 303–311. https://doi.org/10.1016/j.yrtph.2017.03.022

[5] J. Emsley, The elements, Clarendon Press, Oxford (Oxford University Press, New York), (1998)

[6] S. Chałupnik, M. Wysocka, I. Chmielewska, K. Samolej, Radium removal from mine waters with the application of barium chloride and zeolite: comparison of efficiency. J Sustain Min 18 (2019) 174–181. https://doi.org/10.1016/j.jsm.2019.07.002

[7] C.E. Dallas, P.L. Williams, Barium: rationale for a new oral reference dose, J Toxicol Environ Health B Crit Rev, 4 (2001) 395–429. https://doi.org/10.1080/109374001753146216

[8] F. Khalili, A. Mahvi, S. Nasseri, M. Yunesian, B. Djahed, M. Yaseri, Risk assessment of non-carcinogenic heavy metals (barium, cadmium, and lead) in hair color in markets of Tehran, Iran. J. Health Environ, 9 (2016) 27–40.

[9] T. Platzek, Risk from exposure to arylamines from consumer products and hair dyes, Front Biosci (Elite Ed), 2 (2010) 1169–1183. https://doi.org/10.2741/e177

[10] F. Pragst, K. Stieglitz, H. Runge, K.D. Runow, D. Quig, R. Osborne, C. Runge, J. Ariki, High concentrations of lead and barium in hair of the rural population caused by water pollution in the Thar Jath oilfields in South Sudan. Forensic Sci Int 274 (2017) 99–106. https://doi.org/10.1016/j.forsciint.2016.12.022

[11] N. Konduru, J. Keller, L. Ma-Hock, S. Groters, R. Landsiedel, T. C. Donaghey, J. D. Brain, W. Wohlleben, Biokinetics and effects of barium sulfate nanoparticles, Part Fibre Toxicol, 11 (2014) 55. https://doi.org/10.1186/s12989-014-0055-3

[12] T. J. Webster, A. I. Stout, G.E. Yang, Nano-BaSO4: a novel antimicrobial additive to pellethane. Int J Nanomedicine, 8 (2013) 1197-205. https://doi.org/10.2147/ijn.s40300

[13] G. G. Genchi, A. Marino, A. Rocca, V. Mattoli, G. Ciofani, Barium titanate nanoparticles: promising multitasking vectors in nanomedicine, Nanotechnology, 27(23) (2016) 232001. https://doi.org/10.1088/0957-4484/27/23/232001

[14] A. Marino, E. Almici, S. Migliorin, C. Tapeinos, M. Battaglini, V. Cappello, M. Marchetti, G. de Vito, R. Cicchi, F. S. Pavone, G. Ciofani, Piezoelectric barium titanate

ARTICLE IN PRESS

nanostimulators for the treatment of glioblastoma multiforme, J Colloid Interface Sci 538 (2019) 449–461. https://doi.org/10.1016/j.jcis.2018.12.014

[15] G. Crisponi, V. M. Nurchi, J. I. Lachowicz, M. Peana, S. Medici, M. A. Zoroddu, Chapter 18—toxicity of nanoparticles: etiology and mechanisms. In: Grumezescu AM (ed) Antimicrobial nanoarchitectonics. Elsevier, pp (2017) 511–546. https://doi.org/10.1016/B978-0-323-52733-0.00018-5

[16] T. Ketegenov, K. Kamunur, A. Batkal, D. Gani, R. Nadirov, Recent Advances in the Preparation of Barium Sulfate Nanoparticles: A Mini-Review, ChemEngineering 6 (2022) 30. https://doi.org/10.3390/chemengineering6020030

[17] O. Özbek, I.M. Eski, O.C. Altunoluk, Development of a highly selective and ultra–fast potentiometric sensor for thiosulfate detection in water samples. Journal of the Indian Chemical Society, 103 (2026) 102519. https://doi.org/10.1016/j.jics.2026.102519

[18] O. Özbek, O. C. Altunoluk, K. B. Akar, Ö. Isildak. Synthesis, characterization and sensor applications of a new 1,4-naphthoquinone derivative molecule, Chem. Pap, 79 (2025) 3249–3260. https://doi.org/10.1007/s11696-025-04002-x

[19] A. Akyasan, O. Özbek, H. Akbaş, Ö. Işıldak, Protic Ionic Liquid Based Potentiometric Sensors: High Selectivity Detection of Silver (I) Ions, ChemistrySelect, 10 (2025) e202405507. https://doi.org/10.1002/slct.202405507

[20] O. Özbek, O. C. Altunoluk, Potentiometric determination of the local anesthetic procaine in pharmaceutical samples, Anal. Biochem, 695 (2024) 115657. https://doi.org/10.1016/j.ab.2024.115657

[21] E. Kalay, O. Özbek, M. Elik, C. Berkel, O. N. Aslan, The synthesis, sensor and biological properties of two novel rhodanine derivative molecules, J. Indian Chem. Soc, 102 (2025) 101591. https://doi.org/10.1016/j.jics.2025.101591

[22] O. Özbek, O. C. Altunoluk, Ö. Isildak, Surface characterization and electroanalytical applications of the newly developed copper(II)-selective potentiometric sensor, Anal. Sci, 40 (2024) 141–149. https://doi.org/10.1007/s44211-023-00436-z

[23] O. Özbek, M. Elik, Potentiometric determination of anti-inflammatory drug etodolac in pharmaceutical samples and its greenness assessment, Chem. Pap. 79 (2025) 5765–5773. https://doi.org/10.1007/s11696-025-04151-z

[24] O.C. Altunoluk, O. Özbek, E. Kalay, C. Berkel, Ö. Isildak, Synthesis and use of novel rhodanine derivatives to fabricate potentiometric sensors for the determination of toxic heavy metal ions, Microchem J, 218 (2025) 115090. https://doi.org/10.1016/j.microc.2025.115090

ARTICLE IN PRESS

[25] Y. Demirci, E. Kalay, Y. Kara, H. İ. Güler, Z. Can, E. Şahin, Synthesis of Arylsulfonyl Hydrazone Derivatives: Antioxidant Activity, Acetylcholinesterase Inhibition Properties, and Molecular Docking Study, ChemistrySelect, 8 (2023) e202301474. https://doi.org/10.1002/slct.202301474

[26] O. C. Altunoluk, O. Özbek, H. Akbas, Ö. Isildak, Highly selective potentiometric detection of arsenate ions based on newly synthesized protic alkanolammonium ionic liquid, Microchem. J, 213 (2025) 113784. https://doi.org/10.1016/j.microc.2025.113784

[27] O. Özbek, M. E. Cakmak, K. B. Akar, Ö. Isildak, Synthesis, Characterization, and Electrochemical Applications of a New Lawsone Molecule: Potentiometric Determination of Cr (III) Ions with Low Detection Limit, ChemistrySelect, 10(13) (2025) e202500746. https://doi.org/10.1002/slct.202500746

[28] R.P. Buck, E. Lindner, Recommendations for nomenclature of ion-selective electrodes, Pure. Appl. Chem, 66 (1994), 2527–2536. https://doi.org/10.1351/pac199466122527

[29] Y. Umezawa, P. Bühlmann, K. Umezawa, K. Tohda, A.S. Amemiya, Potentiometric selectivity coefficention of ion-selective electrodes, Part I. Inorganic Cations Pure. Appl. Chem, 72 (2000) 1851–2082. https://doi.org/10.1351/pac200072101851

[30] O. C. Altunoluk, O. Özbek, E. Kalay, F. S. Tokalı, O. N. Aslan, Surface characterization of barium(II)-selective potentiometric sensor based on a newly synthesized thiosemicarbazone derivative molecule, Electroanalysis, 36 (2024) e202300407. https://doi.org/10.1002/elan.202300407

[31] S. S. M. Hassan, M. B. Saleh, A. A. Abdel Gaber, K. N. A. Abdel, DDB liver drug as a novel ionophore for potentiometric barium (II) membrane sensor. Talanta, 59 (2003) 161–169. https://doi.org/10.1016/S0039-9140(02)00464-2

[32] A. K. Singh, R. Singh, R. P. Singh, P. Saxena, Novel potentiometric sensor for monitoring barium (II) based on 2, 3, 4-pyridine-1, 3, 5, 7, 12-pentaazacyclopentadeca-3-ene, Sens Actuators B Chem, 106 (2005) 779–783. https://doi.org/10.1016/j.snb.2004.09.030

[33] M. R. Abedi, H. A. Zamani, Barium (II)-PVC membrane sensor based on 4-4′-methylenediantipyrine as a neutral carrier, Anal Lett, 41 (2008) 2251–2266. https://doi.org/10.1080/00032710802238077

[34] A. M. Othman, M. S. El-Shahawi, Abdel-Azeem M, A novel barium polymeric membrane sensor for selective determination of barium and sulphate ions based on the complex ion associate barium (II)–Rose Bengal as neutral ionophore, Anal Chim Acta, 555 (2006) 322–328. https://doi.org/10.1016/j.aca.2005.09.016

ARTICLE IN PRESS

[35] H. A. Zamani, M. T. Hamed-Mosavian, E. Aminzadeh, M. R. Ganjali, M. Ghaemy, H. Behmadi, F. Faridbod, Construction of barium (II) PVC membrane electrochemical sensor based on 3-deoxy-d-erythro-hexos-2-ulose bis (thiosemicarbazone) as a novel ionophore, Desalination 250 (2010) 56–61. https://doi.org/10.1016/j.desal.2009.09.014

[36] O. Özbek, O. C. Altunoluk, Ö. Isildak, Novel solid contact ion selective sensor for potentiometric analysis of barium ions, J Turk Chem Soc B: Chem Eng, 8 (2025) 1–10. https://doi.org/10.58692/jotcsb.1536261

[37] G. Negi, A. S. Goswami-Giri, G. Negi, A. S. Goswami-Giri, Int J Res Eng Appl Sci, 5 (2015) 85–92.

[38] M. B. Saleh, Neutral bidentate organophosphorus compounds as novel ionophores for potentiometric membrane sensors for barium (II), Fresenius J Anal Chem, 367 (2000) 530–534. https://doi.org/10.1007/s002160000374

[39] Y. H. Ma, R. Yuan, Y. Q. Chai, A highly selective polymeric membrane barium(II) electrode based on a macrocyclic tetrabasic ligand as neutral carrier, Anal Bioanal Chem, 395 (2009) 855–862. https://doi.org/10.1007/s00216-009-3029-9

ARTICLE IN PRESS